ELSEVIER

Biophysical Chemistry 56 (1995) 201–214

Biophysical Chemistry

Sequences of actin implicated in the polymerization process: a simplified mathematical approach to probe the role of these segments

Ahmed Houmeida [a,1], René Bennes [a], Yves Benyamin [a,b], Claude Roustan [a,b,*]

[a] *CNRS, UPR 9008 Centre de Recherches de Biochimie Macromoléculaire, INSERM, U. 249, Université de Montpellier 1, France*
[b] *Laboratoire de Recherche sur la Motilité Cellulaire (EPHE), Route de Mende BP 5051 F-34033, Montpellier Cedex, France*

Received 29 March 1994; revised 13 January 1995; accepted 2 February 1995

Abstract

Regulation of actin polymerization and depolymerization is essential for the functions of actin in non-muscle cells and is mediated by a large number of heterologous actin-binding proteins which questions their true impact on the polymerization process. As a model, we report here the modulating effect of monospecific antibody fragments (Fab) as in vitro effectors on actin polymerization kinetics. Polymerization curves were obtained through fluorescence measurements. They were fitted using analytical equations derived from classical models describing the actin polymerization process with the aim of identifying kinetic steps potentially altered by the effectors. The study was limited to three short segments bore by the 300–328 sequence which is located in actin subdomain 3 and implicated in one of the monomer–monomer interfaces. We observed that antibodies which inhibited actin polymerization reacted with both G-and F-actins, modulated both nucleation and elongation steps, enhanced actin monomer dissociation from the filament and apparently did not act as capping or sequestering proteins. Among the antibody populations specific for a restricted and selected sequence in subdomain 3 of actin (sequence 300–326), only those directed to epitopes located near Met 305 and 325 were effective. In contrast, antibodies directed towards the α-helix located between the two preceding epitopes had no effect. All the results analyzed here emphasize the important role of some discrete regions and their conformational state in regulation of the interconversion between monomeric and polymeric actins which could be controlled in different ways by the various actin-binding proteins.

Keywords: Actin, Polymerization process, Specific antibodies

Abbreviations: Nbd-Cl: 7-chloro-4-nitrobenzo-2-oxa-1,3-diazole; Oxa: performic acid-treated actin; Buffer A: 140 mM NaCl/50 mM Tris buffer, pH 7.8 supplemented with 0.5% gelatin/3% gelatin hydrolyzate.

* Corresponding author. Centre de Recherches de Biochimie Macromoléculaire (CNRS), route de Mende, BP 5051, F-34033 Montpellier Cedex, France.

[1] Present address: Department of Veterinary Medicine, Churchill Building, Langford, Bristol, UK.

SSDI 0301-4622(95)00038-0

1. Introduction

Actin polymerization is a fundamental process occurring in the presence of cations (i.e. Mg^{2+} and K^{+}) and allowing formation of non-covalent helical filaments (F-actin). Mechanisms of this process have been widely studied. The actin monomer binds one molecule of ATP which is hydrolyzed into ADP during the polymerization process. Elongation is the result of specific interactions of G-actin at both ends of the growing filaments. In addition, conformational differences between monomeric and filamentous actins have already been observed, namely by UV difference spectra [1], by comparing initial rates of proteolytic digestion [2] and antigenic reactivities [3]. Recent data on F-actin structure [4,5] have shown the occurrence of extensive interactions between actin molecules along the two-start actin helix. The 300–328 sequence in subdomain 3 of actin is one of the segments which could be involved in these interfaces [4]. This sequence presents two loops adjacent to a central α-helix which incorporates residues 309–320 [6]. More precisely, its C-terminus is located near a loop (243–245 sequence) in the adjacent actin molecule, while its N-terminus is located around adenine ring [6]. Furthermore, this part of the actin sequence displays a large temperature factor suggesting a rather flexible structure [6].

In the same period, a great number of studies identified various actin binding proteins which interacted with the subdomain 3 of actin and influence the polymerization kinetics by stabilizing the actin filament (i.e., tropomyosin, scruin) [7] or by inducing polymerization (i.e., myosin head) [8], monomer sequestration (i.e., profilin) [9] or filament severing (i.e., gelsolin) [10].

The above considerations prompted us to test well-defined effectors which affect, by their interactions with the 300–326 sequence, the G–F actin equilibrium and could mimic the effects of actin binding proteins on actin polymerization. We report here mathematically studies designed to define critical segments in this sequence and to identify the step(s) which were concerned in the polymerization kinetics. In this way, we analyzed the effect of different antibodies and their related Fab fragments specific for this limited region of actin.

2. Material and methods

2.1. Proteins

Rabbit skeletal muscle and scallop (*Pecten maximus*) muscle actins were purified from acetone-dried powder [11]. Actin was specifically labelled at Lys

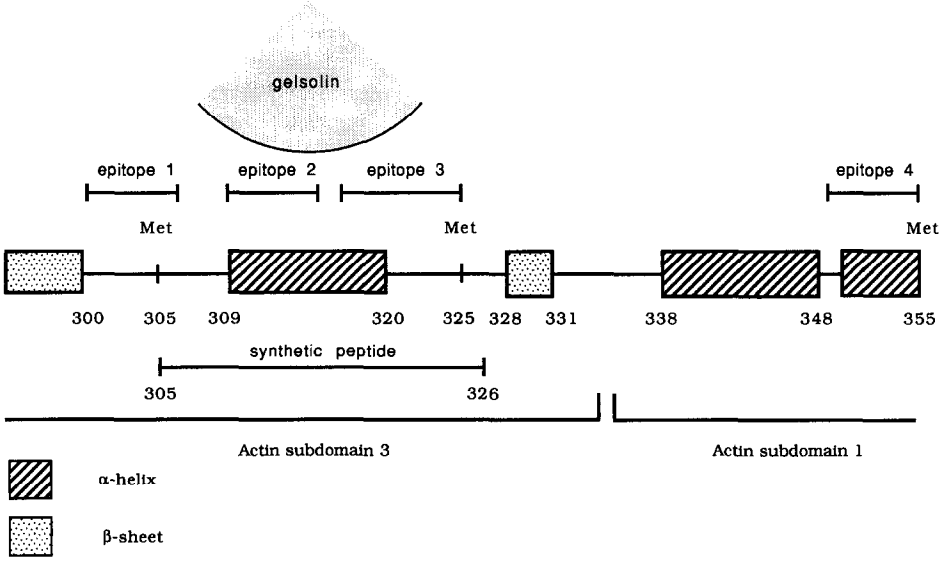

Fig. 1. Location of antigenic epitopes on the actin sequence.

373 with 7-chloro-4-nitrobenzo-2-oxa 1,3 diazole (Nbd-Cl) or at Cys 374 with N-pyrenyl iodoacetamide [12,13]. The 305–326 actin fragment was synthesized on a polyacrylamide-based support (Expansine, Expansia, Aramont, France) as previously described [14]. Bovine plasma gelsolin was purified as described by Soua et al. [15]. Proteins concentrations were determined by UV absorbance [16].

2.2. Antibodies

Antiserum to peptidyl-resin of sequence 305–326 was elicited in rabbits by direct injection of the crushed peptidyl-resin emulsified in Freund's adjuvant as previously described [17]. The antibodies (anti-(epitope 2) antibody) were purified by affinity chromatography on a rabbit skeletal S-carboxymethylated-actin column [18]. They showed a good reactivity to the coated peptide as well as to G-or F-actin [14,19] demonstrating the accessibility of the epitope in the native actin in accordance with the three-dimensional structure [5,6].

Antiserum to performic acid-treated actin (Oxa) from rabbit skeletal muscle was raised in sheep [18]. The antiserum presented reactivity towards two major epitopes, one including residue 201 and another within the 226–375 actin fragment [3,18,20]. The last epitope has been restricted, by using synthetic peptides, in the 305–326 sequence [21]. Therefore, the corresponding antibody subpopulation (anti-(epitope 3) antibody) (Fig. 1) was extracted from this antiserum on a peptidyl-resin (sequence 305–326) column.

Antiserum which specificity is directed against epitopes 1, 3 and 4 (anti-(epitopes 1, 3, 4) antibodies) was induced in sheep [18], using fragment 285–375 from rabbit skeletal muscle coupled to haemocyanin as antigen [22]. Its specificity was previously located on actin sequence [23,24]. The corresponding antibodies presented activity to epitopes 1, 3, and 4 including Met 305, 325 and 355 respectively (Fig. 1). The specificity was checked by direct ELISA and by competition experiments using actin isoforms and various peptides derived from actin. These antibodies were initially purified on a column of S-carboxymethylated actin from rabbit skeletal muscle [18]. This preparation was then further purified into two subpopulations using the occurrence of mutations in scallop versus rabbit skeletal muscle actins in the epitope 1 [25,26]. For this, the antibody preparation was passed down a column of S-carboxymethylated actin from scallop muscle. The subpopulation reactive against epitope 1 did not bind on the column. The antibody subpopulations to epitopes 3 and 4 were retained on the matrix and then eluted at pH 12 in the presence of 10% dioxane [27,28]. In particular, this procedure allowed us to obtain, although in small quantities, a purified monospecific antibody directed to epitope 1. All the purified antibodies used in this study displayed similar reactivity towards both G-and F-actins [21,24].

Antibody directed to sequence 1–7 of actin was obtained as previously described [18]. Fab fragments were obtained after papain digestion [29]. Anti-IgG antibodies labelled with alkaline phosphatase were purchased from Biosys (Compiègne, France).

2.3. ELISA

Interactions between antibodies and actin or peptides were studied by direct ELISA as previously described [30]. Briefly, actin and peptides were coated on the plastic of microtiter plate wells by incubation in 50 mM $NaHCO_3/Na_2CO_3$, pH 9.5, overnight at 4°. Unoccupied protein-binding sites were saturated in 140 mM NaCl/50 mM Tris buffer, pH 7.8, supplemented with 0.5% gelatin/3% gelatin hydrolyzate (buffer A). Antibody dilutions were also performed in buffer A. Binding was revealed with alkaline phosphatase labelled anti-IgG antibodies diluted to 1/3000. After washing, a solution of *p*-nitrophenylphosphate (1 mg/ml) was added and staining was read at 405 nm. Non-specific absorption was determined for each sample using uncoated wells. Each experiment was conducted in triplicate and the results were analysed by nonlinear fitting. In order to study the effect of magnesium on F-actin conformation, direct ELISA was done as follows: each well was coated with 50 μg of filamentous actin polymerized in the presence of 2 mM $MgCl_2$, 0.1 mM ATP. The coated plates were washed with 50 mM Tris buffer, pH 7.2 supplemented with 0 to 0.5 mM $MgCl_2$ and incubated for 15 min. After addition of the same buffer of the chosen anti-actin antibody to the incubation mixture, the assay was carried out as described above.

In indirect ELISA, a fixed concentration of an antibody was reacted in the presence of increasing concentrations of the other one to shift the equilibrium. Other experimental details are mentioned in the figure legends.

2.4. Actin polymerization

The polymerization of actin was followed either by fluorescence or ultracentrifugation. Fluorescence measurements were carried out using a Kontron 25SFM fluorescence spectrophotometer or a Perkin-Elmer Luminescence Spectrometer LS-50. Fluorescence enhancement of Nbd-actin or pyrenyl-actin was used as an indicator of actin polymerization [31–33]. The excitation and emission wavelengths were set at 480 nm and 545 nm respectively for Nbd-actin and at 355 and 386 nm respectively for pyrenyl-actin. Polymerization was induced by adding 2 mM $MgCl_2$, 0.1 M KCl. In some experiments, extrapolation of the polymerization time-course at $t = \infty$ was calculated as described in Fesce et al. [34].

Co-sedimentation experiments were conducted in a Beckman Airfuge [26,35]. A 100 μl sample containing G-actin (300 μg) was incubated for 40 min at 25°C in the presence of various antibody concentrations before adding 2 mM $MgCl_2$, 0.1 M KCl. After polymerization, the mixture was centrifuged for 20 min at 30 psi. 30 μl of the supernatant was removed and analyzed by SDS-PAGE [36].

3. Results

3.1. Three targets in the 300–326 actin sequence

We first investigated, by using ELISA, the activity of several antibodies, which specificity to precise regions of the COOH-terminal part of actin (Fig. 1) has been previously demonstrated, in order to obtain precise information on the mutual location of antigenic determinants within the 300–326 sequence. The relative locations between anti-(epitope 2) antibody elicited by the peptide-resin of sequence 305–326 and the anti-(epitopes 1, 3, 4) antibodies raised against the fragment 285–375 (directed against sequences including residues 305, 325 and 355; epitopes 1, 3 and 4, respectively) [23,24] were determined. We first observed that both antibody preparations interacted with the synthetic peptide of sequence 305–326 (Fig. 2). In further experiments, the microtiter plate wells were coated with the synthetic peptide-resin (305–326 sequence) and the anti-(epitopes 1, 3, 4) antibodies were reacted in the presence of increasing concentrations of the anti-(epitope 2) antiserum. The results reported in Fig. 3A show that the two antibodies afforded only very partial competition towards the 305–326 sequence. So epitopes constitute close but different sequences with independent antigenic reactivities. Further information on the precise location of these epitopes was obtained by studying the simultaneous interactions with coated G-actin of anti-(epitope 2) antibody and the subpopulation of anti-(epitopes 1, 3, 4) antibodies specific to epitope 1 (see Material and methods), because this last population does not react with the 305–326 sequence (Fig. 2). Fig. 3B shows that the anti-(epitope 2) antibody reactivity was not altered at all in the presence of anti-(epitope 1) antibody. From these results, we concluded that the binding site for the anti-(epitope 2) antibody was located between epitope 1 and epitope 3 (Fig. 1). This intermediate region (including epitope 2) corresponds to an α-helical part in the three-dimensional structure of actin [6], the two other epitopes being supported essentially by loops located at the two ends of the α-helix. So, this actin region, located at the surface of subdomain 3, bore three epitopes showing independent antigenic reactivities.

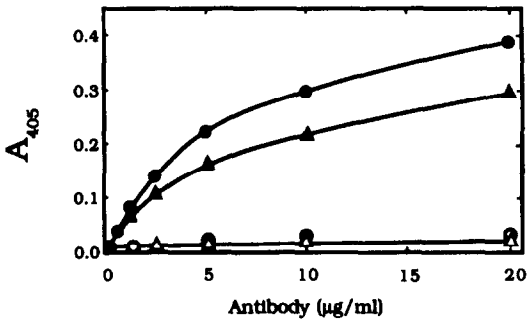

Fig. 2. Reactivity of anti-actin antibodies to the synthetic peptide (305–326) of actin coupled to resin revealed by ELISA. Reactivity towards coated synthetic peptide resin (10 μg/ml of peptide/well) of anti-(epitopes 1, 3 and 4) (●), anti-(epitope 1) (○) and anti-(epitope 2) (▲) antibodies. Anti-(epitope 2) antibody (△) was reacted with coated resin alone as standard.

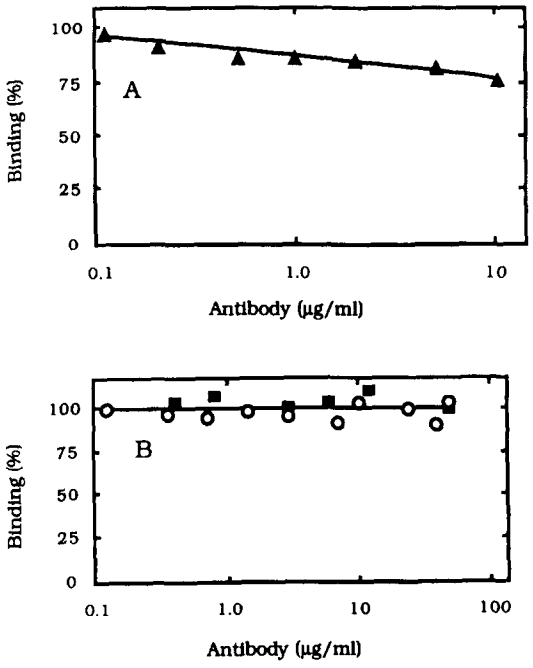

Fig. 3. Interdependence of anti-actin antibody reactivity revealed by ELISA. (A) Competitive binding between anti-(epitopes 1, 3 and 4) and anti-(epitope 2) antibodies. Anti-(epitopes 1, 3 and 4) antibodies were incubated with the synthetic peptide (305–326) of actin coupled to resin (coated at 10 µg of peptide/well) in the presence of increasing concentrations of anti-(epitope 2) antibody. (B) Binding of anti-(epitope 2) antibody with G-actin (coated at 100 ng/well) in the presence of increasing concentrations anti-(epitope 1) (○) or anti-(epitope 3) (■) antibody populations.

The (anti-(Oxa) antibody subpopulation (anti-(epitopes 3) antibody) raised against performic acid-treated actin and purified on the 305–326 peptide by affinity chromatography also reacted with the epitope 3 (near Met 325) as assessed by its strong competition with anti-(epitope 3 + 4) antibodies [21]. From its location far from the 300–326 sequence in the actin structure (subdomain 1 of actin) [6], epitope 4 was not involved in this competition. In addition, the anti-(epitope 3) antibody did not compete (Fig. 3B) with anti-peptide antibody (epitope 2). Direct ELISA experiments (see Material and methods) give an apparent Kd of about 24 nM for (anti-(epitopes 3) antibody) towards G-and F-actins.

We thus characterized and purified three independent antibody populations covering the 300–326 sequence (Fig. 1) which can be used in the detection

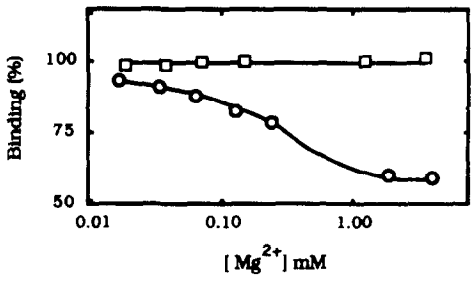

Fig. 4. Mg^{2+} effect on immunoreactivity of anti-(epitope 1) (○) and anti-(1–7) (□) antibodies revealed by ELISA. Antibodies were tested against filamentous actin (coated at 50 µg/well) in the presence of increasing Mg^{2+} concentrations.

and location of conformation changes in this part of actin structure or used as tools to induce alterations in the actin polymerization process. These specific antibody populations and their related Fab fragments were used in all subsequent experiments.

3.2. *Identification of a conformational change induced by Mg^{2+} interaction at low binding sites*

The purified antibody populations described above were then used in ELISA to monitor the antigenic activity of F-actin (see Material and methods) in the presence of increasing magnesium concentrations. When these concentrations varied from 0.05 to 2 mM, we observed that the interaction of anti-(epitopes 1, 3, 4) antibodies with filamentous actin is markedly weakened by the presence of Mg^{2+} as described by Mejean et al. [24]. The effects of magnesium on each of the antibody subpopulation directed to the 300–355 sequence of actin were then studied. Among the populations tested (directed to epitopes 1, 2, 3 and 4), only antibodies specific to epitope 1, corresponding to a region located near

Table 1
Interaction of specific anti-actin antibody subpopulations with F-actin in the presence of Mg^{2+} (2 mM)

Antibody	Loss of reactivity (%)
Anti-epitope (1)	45 ± 5
Anti-epitope (2)	0
Anti-epitope (3)	0
Anti-epitope (3 + 4)	0

Met 305, showed a large decrease in binding (45–50%) (Fig. 4 and Table 1). The maximal effect was obtained at about 2 mM Mg^{2+} and was detectable at 0.1 mM. This range of concentrations can be ascribed to the interaction of Mg^{2+} with the weak metal binding sites in actin. Ca^{2+} at the same concentrations was without effect [24]. In addition, anti-(1–7) antibody specific to the N-terminal sequence of actin whose reactivity is not modified by Mg^{2+} [24] were used as a control (Fig. 4). This negative control gave evidence that the presence of 2 mM Mg^{2+} is unable to affect by a direct way (electrostatic neutralization or ionic strength increasing) the antigenic activity of the N-terminal negatively charged cluster of actin. So the detected effect after addition of Mg^{2+} on the uncharged 300–307 sequence (epitope 1) is certainly due to Mg^{2+} conformational changes after saturation of low affinity cation binding sites. In conclusion, a conformational reorganization of the actin subdomain 3, namely the 300–307 sequence, is due to the divalent cation Mg^{2+}.

3.3. Actin polymerization process, a simplified mathematical analysis

The kinetics of actin polymerization and related molecular mechanisms of nucleation and elongation have been extensively investigated and many reviews published [37–39]. However, the aim of this analysis was to obtain a simplified description of the time-course of actin polymerization and kinetic parameters to characterize the process and its modification by the interaction of proteic effectors. The equations developed here were fitted by iteration search (Marquartd algorithm; UltraFit software, Biosoft) of the experimental curves.

We started from the usual nucleation and elongation equilibria [32]:

(a) nucleation: $A_{n-1} + A_1(k^+/k^-)A_n$, with $K_{n-1} = [A_1]^{n-1}/[A_{n-1}]$

(b) elongation: $A_n + A_1(k^+/k^-)A_{n+1}$, where A_1 = free actin, A_n actin nuclei, k^+ and k^- = forward and backward rate constants, respectively.

In fact, as elongation can occur at the barbed and pointed ends of the filament, rate constants corresponded to the sum of the individual constants [37].

Elongation can thus be written as:

$$-\mathrm{d}A_1/\mathrm{d}t = k^+C(A_1 - A_1^\infty) \quad (1)$$

and the kinetics of nucleation:

$$\mathrm{d}C/\mathrm{d}t = K_{n-1}k^+A_1^{n-1}(A_1 - A_1^\infty) \quad (2)$$

where $C = A_n$ = nuclei concentration, $A_1^\infty = k^-/k^+$ and t = time.

By elimination of $A_1 - A_{1\infty}$ and integration, we note first that the relation between the nuclei concentration C and the free actin concentration A_1 is:

$$C = \left[(A_{1T}^n) - A_1^n)2K_{n-1}/n\right]^{1/2} \quad (3)$$

where A_{1T} = total actin concentration and n = number of actin molecules into the nuclei, which was fixed at 4 according to [33,34].

Approximate solution for Eq. (2) for $A_1 \gg A_1^\infty$

By combining Eqs. (2) and (3), we obtain a differential equation for C which can be easily solved as $C = C_m \tanh K't$ (Eq. (4)), with:

$$C_m = k^+(K_{n-1}A_{1T}^n 2/n)^{1/2} \quad (5)$$

$$K' = k^+(K_{n-1}A_{1T}^n n/2)^{1/2}. \quad (5')$$

A combination of Eqs. (3), (4) and (5) gives the free actin concentration versus time for the approximation $A_1 \gg A_1^\infty$:

$$A_1 = A_{1T}(\cosh K't)^{-2/n} \quad (6)$$

Approximate solution for Eq. (1) for $A_1 \to A_1^\infty$ $(t \to \infty)$

First, we can say that the nuclei concentration has raised its maxima value, i.e. $C = C_m$. The result is

$$A_1 = A_1^\infty + (A_{1T} - A_1^\infty)\exp[-K(t-\tau)] \quad (7)$$

where $K = (2/n)K'$ or $K = k^+C_m$ (Eq. (7')), τ being defined as $t = \tau$ when $A_1 = A_{1T}$.

Establishment of the general equation

First, we note that for $t \to \infty$, $\cosh K't \to 1/2 \exp(K't)$; as $(2/n)K' = K$, $(\cosh K't)^{-2/n} \to (1/2)^{-2/n} \exp(-Kt)$. The general equation which describes the whole A_1 versus t curve is:

$$A_1 = A_1^\infty + (A_{1T} - A_1^\infty)(\cosh K't)^{-2/n} \quad (8)$$

which is very similar to that proposed by Fesce et al. [34]. In conclusion, we can note that:

—the significance of τ is straightforward: $\tau = (2/nK)\ln 2$;

—Eqs. (7) and (8) can be resolved by a fit to determine parameters K or K';

—knowing K', Eq. (4) gives the shape of the per cent of formed nuclei versus time;

—if the model is correct, K' or K is proportional to $A_{1T}^{n/2}$.

The limitation of the model may came from the major hypothesis made, i.e., k^+ and k^- relative to elongation are identical to k^+ and k^- relative to nucleation as in the classical model developed by Tobacman and Korn [33]. Consequently all deviation observed on k_{n-1} shall be transferred to k^-.

3.4. Effect of the anti-(epitopes 1, 3, 4) antibodies on the actin polymerization process

The rate and extent of actin polymerization induced by 2 mM $MgCl_2$ and 0.1 M KCl, in the presence of the purified polyclonal antibodies specific to epitope 1, 3 and 4 (anti-(epitopes 1, 3, 4) antibodies) were followed through fluorescence changes in either NBD-or pyrene-labelled actins. Analysis of the polymerization kinetics gave similar results for the two fluorescent actins.

Fig. 5 shows that anti-(epitopes 1, 3, 4) antibodies used at several concentrations had a strong inhibitory effect on actin polymerization. In particular, as shown

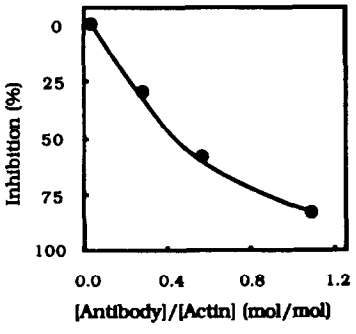

Fig. 5. Effect of anti-(epitope 1, 3 and 4) antibodies on the rate of actin polymerization. Polymerization of Nbd-actin (6.35 μM) was followed by fluorescence. The exitation and emission wavelengths were set at 480 and 545 nm, respectively. Inhibition (%) is plotted versus antibody/actin ratio.

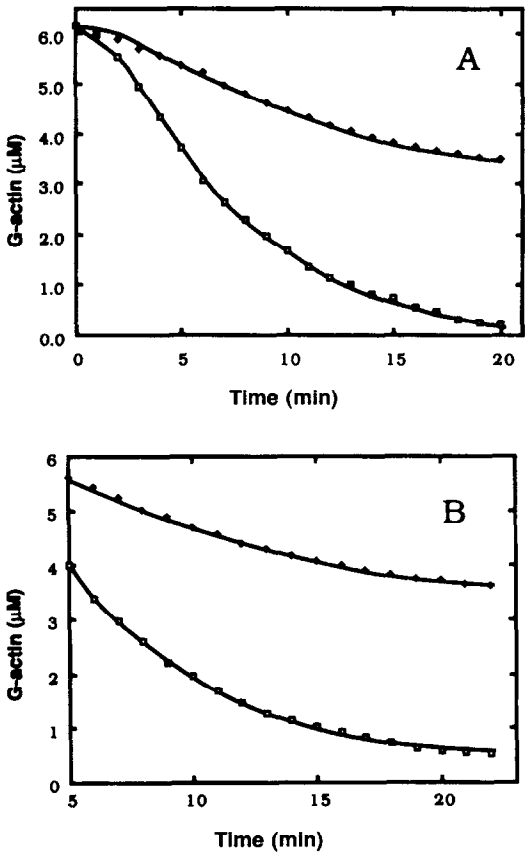

Fig. 6. Progress curves showing Nbd-actin polymerization induced by 2 mM $MgCl_2$ and 100 mM KCl in the absence (□) or in the presence (♦) of anti-(epitope 1, 3 and 4) antibodies (antibodies/actin molar ration of 0.56). Polymerization of Nbd-actin was followed by fluorescence. The exitation and emission wavelengths were set at 480 and 545 nm, respectively. Measurements were carried out in 2 mM Tris/HCl buffer, pH 7.6 containing 0.2 mM ATP and 0.1 mM $CaCl_2$. In A and B, residual G-actin concentrations were plotted versus time. The experimental results were fitted using Eq. (8) in A and (7) in B. This analysis gave the following values for the kinetic constants : actin alone $K = 0.148\ min^{-1}$, $K' = 0.300\ min^{-1}$ and $A_1^{\infty} = 0.20\ \mu M$, in the presence of antibodies $K = 0.105\ min^{-1}$, $K' = 0.220\ min^{-1}$ and $A_1^{\infty} = 3.10\ \mu M$.

in Fig. 6 where free G-actin was followed, they reduced both the polymerization rate and the extent of actin association. Fig. 6A and Fig. 6B also present an analysis of experimental data using Eqs. (8) and (7). In addition it is interesting to note that similar results were obtained when the extent of polymerization was determined either after extrapolation (see

Material and methods) or by direct measurement after a sufficient time (several hours). In a control experiment, we found that antibody binding did not modify fluorescence of the labelled actins (data not shown). The decrease observed in the maximum fluorescence after polymerization can thus be ascribed to the inhibitory effect of the antibodies. The decrease in the extent of polymerization was also confirmed by ultracentrifugation (Table 2). In addition, because of the bivalent nature and the bulk of the antibodies (IgG), the inhibition of polymerization was also studied by using Fab fragments. Similar results were obtained with entire antibodies or with their related Fab fragments (Fig. 7) showing that the hypothesis of a steric blocking of the monomer–monomer interaction is unlikely.

The decrease in the maximum amounts of F-actin produced during polymerization can be tentatively ascribed either to the sequestration of monomeric actin by antibodies, as reported for vitamin-D-binding protein [40], or to an alteration in the rate constants describing the polymerization process. To test the first hypothesis, we performed these kinds of experiments.

First, the effect of increasing concentrations of antibodies on the K constant defined as k^+C_m was studied. In such a case of a sequestering mechanism a part of the monomeric actin could be complexed and sequestered by the antibodies and only the free actin monomers would be implicated in the filament formation. If this hypothesis is verified, we would obtain a linear correlation (see Eqs. (5′) and (7′)) between the square of the total free monomeric actin concentration and the K constant as observed for actin alone at various concentrations (Fig. 8A). Fig. 8B clearly shows that there was no linear correlation.

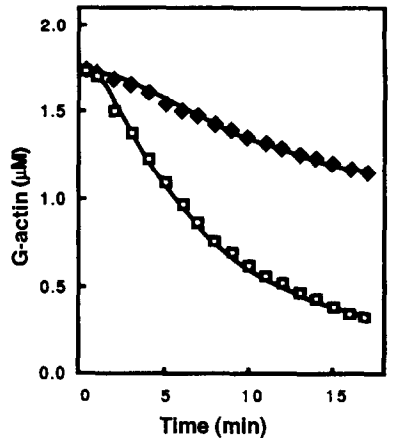

Fig. 7. Progress curves showing Nbd-actin polymerization induced by 2 mM $MgCl_2$ and 100 mM KCl in the absence (□) or in the presence (♦) of anti-(epitope 1, 3 and 4) Fabs (Fab/actin molar ration of 1.3). Polymerization of Nbd-actin (1,74 µM) was followed by fluorescence as described in Fig. 6. The experimental results were fitted using Eq. (8). This analysis gave the following values for the kinetic constants: actin alone $K' = 0.033\ min^{-1}$ and in the presence of Fab $K' = 0.021\ min^{-1}$.

Secondly, we determined the repartition of the antibodies between the pellet and the supernatant in ultracentrifugation experiments (see Material and methods). We observed that, after completion of actin polymerization performed in the presence of anti-(epitope 1, 3, 4) antibodies, incorporation of the antibodies in the filament occurred (Table 2).

We can therefore conclude from these two approaches, that the actin–antibody complex copolymerized with free actin and therefore was incorporated in the filaments but at a slower rate. Accordingly, Fig. 9 shows a decrease in the rate of nuclei formation. Therefore, the effect of antibodies on the elongation process was separately tested by studying F-actin formation from preformed gelsolin–actin complex to bypass the nuclei formation step [41]. Then we observed a substantial modification in the extent of polymerization, but only a slight variation in the kinetic K constant (Fig. 10). Therefore, in our experimental conditions, in which C_m is fixed and K is not strongly affected by the presence of antibodies, we observed an increase in the A_1^∞, suggesting a rise

Table 2
Co-sedimentation of anti-(epitopes 1, 3, 4) antibodies with F-actin [a]

Experiment	Actin (µg/ml)		Antibodies (µg/ml)	
	Supernatant	Pellet	Supernatant	Pellet
1	–	–	98	02
2	49	51	60	40
3	71	129	64	36

[a] Actin (0, 100, 200 µg/ml in experiments 1, 2 and 3, respectively) was polymerized for twenty hours in the presence of antibodies as described in Material and methods. The mixture was centrifugated for one hour at 100000g, and the pellets and supernatants subjected to slab gel electrophoresis and quantified after integrations.

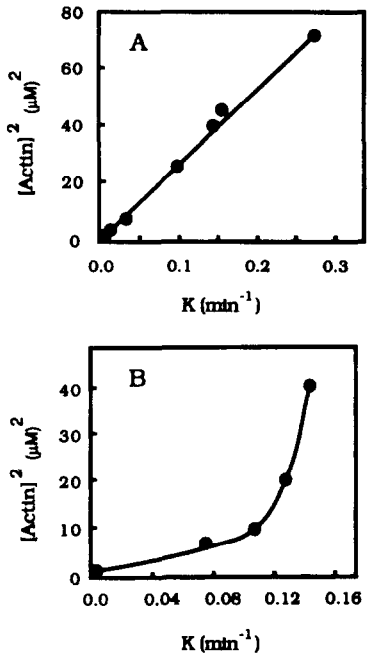

Fig. 8. Correlation between the kinetic constant K and the total actin concentration A_{1T}. (A) Polymerization of Nbd-actin performed in the absence of antibodies. The square of total actin concentration is plotted versus K according to Eqs. 5′ and 7′. (B) Polymerization of Nbd-actin performed in the presence of various anti-(epitope 1, 3 and 4) antibody concentrations. Similarly, the square of actin concentrations, not complexed with the antibody, is plotted versus K.

in the rate constant k^-. In addition, the effect of antibodies on preformed actin filaments was investigated and the results are shown in Fig. 11. In this study, F-actin was diluted 20–40-fold by mixing

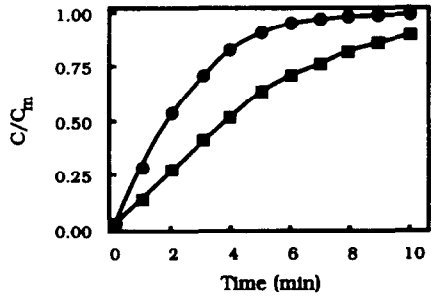

Fig. 9. Effect of anti-(epitope 1, 3 and 4) antibodies on the nucleation step of actin polymerization. Variation of C/C_m versus time is traced from Eq. 4 using the kinetic parameters determined in Fig. 5. The curves were calculated in the presence (■) and absence (●) of anti-(epitope 1, 3 and 4) antibodies.

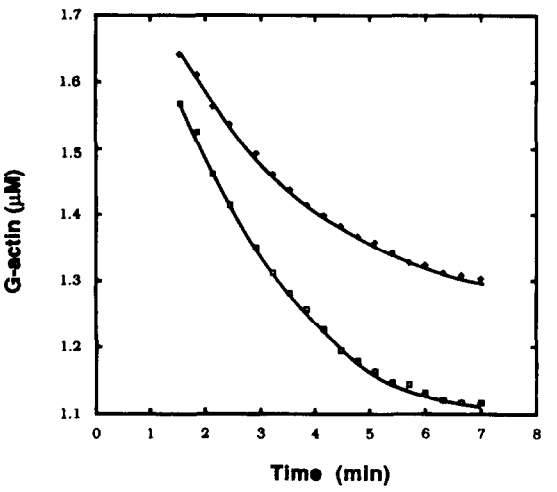

Fig. 10. Effect of antibodies on the elongation step. Pyrenyl-actin (1.75 μM) was capped with gelsolin (0.07 μM) before polymerization by 2 mM $MgCl_2$, 100 mM KCl in the absence (□) or presence (♦) of anti-(epitope 1, 3 and 4) antibodies (antibody/actin molar ratio 0.67). Polymerization of labelled actin was monitored by fluorescence. The experimental data, plotted as residual monomeric actin concentrations versus time, were fitted using Eq. (7). The corresponding kinetic constants were for actin alone, $K = 0.460\ \text{min}^{-1}$ and $A_1^\infty = 1.09$ mM and in the presence of antibodies, $K = 0.435\ \text{min}^{-1}$ and $A_1^\infty = 1.29$ mM.

with solutions containing anti-(epitope 1, 3, 4) antibodies (in 2 mM Tris, 0.1 mM $CaCl_2$, 0.1 mM ATP, 0.1 M KCl, 2 mM $MgCl_2$ buffer, pH 7.5). In the absence of antibodies, the depolymerization of actin which occurred upon dilution resulted from the dissociation of actin monomers apart the filament ends to restore the critical monomeric concentration. From Eq. (1) we can write: $(dA_1/dt)_{t=0} = A_1^\infty k^+ F_0 = k^- F_0$, where F_0 is the concentration of filaments at $t = 0$. Therefore:

$$(dA_{1F}/dt)_{t=0} = -k^- F_0 \qquad (9)$$

where A_{1F} = actin concentration in the filaments. Eq. (9) allows us to compare the initial rates of depolymerization in the presence or absence of the inhibitor. We observed that the addition of the antibodies accelerated the depolymerization rate (Fig. 11). The antibodies would directly interact with F-actin and promote the disassembly of actin monomers by increasing the rate constant of dissociation k^-. In conclusion, anti-(epitopes 1, 3, 4) antibodies inhib-

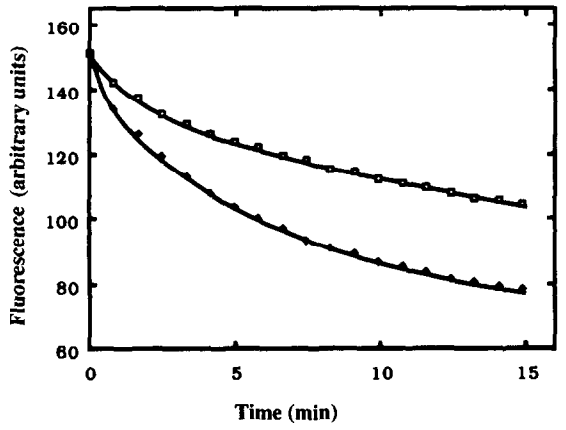

Fig. 11. Effect of antibodies on actin depolymerization. Pyrenyl-F-actin (10 μM) in 2 mM Tris/HCl, 0.2 mM ATP, 0.1 mM $CaCl_2$, 2 mM $MgCl_2$, 100 mM KCl buffer, pH 7.6 was quickly diluted to 0.5 μM in the absence (□) or presence (♦) of anti-(epitope 1, 3 and 4) antibodies (0.37 μM) and the decrease in fluorescence followed versus time. Initial velocity was 2-fold enhanced in the presence of the antibody.

ited actin polymerization without sequestering a pool of monomeric actin.

3.5. *The target of the inhibitory antibody*

A more precise location of the sites concerned with the inhibition described above was obtained by using purified monospecific antibodies. Therefore, anti-(epitope 1) antibody was derived from the anti-(epitopes 1, 3, 4) immunoserum, anti-(epitope 3) from anti-(Oxa) immunoserum and anti-(epitope 2) antibody from the immunoserum elicited by the synthetic peptide of sequence 305–320 (see Material and methods). The selected monospecific antibody populations were reactive towards epitopes 1, 2 and 3, respectively, as indicated in Fig. 1 and covered the 300–326 actin sequence. Dependence of polymerization inhibition on antibody/actin ratio is reported in Fig. 12. Each of the two populations specific to actin

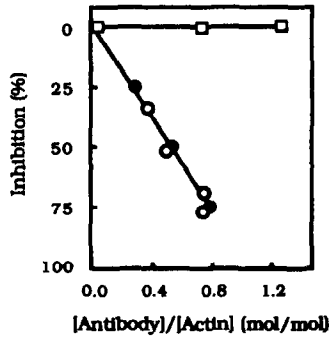

Fig. 12. Effect of different monospecific anti-actin antibody populations on the rate of Nbd-actin polymerization. (●) Anti-(epitope 1), (□) anti-(epitope 2) and (○) anti-(epitope 3) antibody populations Inhibition (%) is plotted versus antibody/actin ratio.

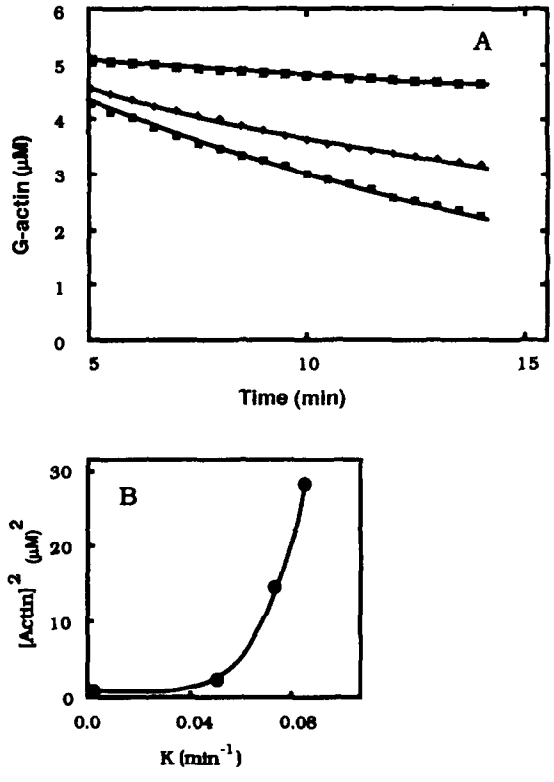

Fig. 13. Effect of anti-(epitope 3) antibody population on actin polymerization. (A) Progress curves showing Nbd-actin (5.35 μM) polymerization induced by 2 mM $MgCl_2$, 100 mM KCl in the absence (■) or in the presence of anti-(epitope 3) antibody (♦) (antibody/actin molar ratio of 0.33), (□) (antibody/actin molar ratio of 0.75). Experimental values were fitted using equation 7. Analysis gave $A_1^\infty = 0.2$ mM for actin alone, 1.75 μM and 3.95 μM for antibody/actin ratios of 0.33 and 0.75, respectively. (B) Polymerization of Nbd-actin performed in the presence of several anti-(epitope 3) antibody concentrations. Square of actin concentrations, not complexed with antibodies, is plotted versus K as in Fig. 8.

sequences near Met 305 (epitope 1) and Met 325 (epitope 3) appeared to be effective. In this latter case, punctual experiments reported in Fig. 13 show a similar inhibitory pattern as observed above for anti-(epitopes 1, 3, 4) antibodies. Namely, anti-(epitope 3) antibody interaction reduced polymerization rates and extents of F-actin formation (Fig. 13A) Furthermore, the effect of antibody concentration on the K constant was studied (Fig. 13B) and gave a non linear relation suggesting as for anti-(epitopes 1, 3, 4) antibodies incorporation in the filament of both actin complexed with antibodies and free actin monomers. In contrast, the antibody population directed against epitope 2 located between Met 305 and Met 325 did not affect the actin polymerization.

4. Discussion

Actin polymerization is induced and modulated by salts and a large number of protein effectors (for a review, see [42]). These proteins can strongly affect kinetic parameters of the different steps of the polymerization process. Earlier steps in the assembly of monomeric actin, particularly nucleation, are often implicated in these regulations. For example, gelsolin cross-links two actin monomers and therefore accelerates the actin polymerization rate in the presence of salts [43]. In contrast, the binding of associated proteins such as vitamin-D-binding protein to actin monomers abolishes the self association of actin into filaments [43]. Similarly, aginactin, a heat-shock protein [44], strongly inhibited actin polymerization through a barbed-end capping mechanism [45].

Conversely, polymerization induced by the myosin head in the absence of divalent cations might result from conformational changes in the actin molecule produced by the interaction of S1 with each monomer [46].

The approach developed here was aimed at obtaining direct correlations between precise sequential segments on an restricted actin surface in subdomain 3 and changes in the polymerization parameters. To this end, we have developed a simplified description of the time course of actin polymerization. In fact this process is very complex and involved many equilibrium and kinetic steps. Their modeling needs a too great number of differential equations to be mathematically easily solved. In this study, we started from classical simplified models [32,37,38] to derive analytical functions allowing to describe experimental data by standard methods of curve fitting. This analytical approach can be used to evidence changes in the kinetics of the polymerization induced by the binding of antibodies to actin. We used purified antibodies as specific effectors whose specificity towards small actin sequences in the 305–326 sequence was precisely determined [17,18,21,23,24]. In fact, antibodies appeared useful as they present a contact interface area with antigens (1250–1950Å^2) which is in the range observed for actin binding protein interfaces such those found in DNAse-1 (1830 Å^2) and profilin (2250 Å^2)-actin complex [9,47]. Here, we focused our study on epitopes located in the 300–326 sequence in subdomain 3 of actin since this flexible region of 27 residues corresponds to one of the binding site of gelsolin an important regulator of polymerization process [14]. A very important feature of the antibodies used here concerned their similar reactivity towards both monomeric and filamentous actins as previously determined [21,24]. Therefore the amino acid residues implicated in the antigenic epitopes are not directly concerned with the monomer–monomer interfaces in the filament.

The interaction between an effector such as an antibody molecule and actin can affect the monomer–polymer equilibrium in actin by either enhancing or inhibiting the extent and rate of polymerization. For example, Dasgupta et al. [48] have reported that their antibodies specific to a sequence in the N-terminal of actin accelerates the polymerization rate. In particular, they shorten the initial lag phase which is classically associated with the nucleation step. In contrast, two of the three antibody or Fab derived populations used in this study and directed to epitopes located in the 300–326 sequence strongly inhibited polymerization, the third one being without any effect. They are respectively in interaction with the two loops (sequences 300–309 and 321–328) and the central α-helix (sequence 310–320) characteristic of this actin region (Fig. 1).

Analysis of the effects of antibodies or Fab fragments on the kinetic parameters describing the polymerization process showed that their interactions with monomeric actin strongly affected both the nucle-

ation and elongation steps and shifted the monomer–polymer equilibrium. This interpretation is essentially substantiated by the following observations.

We obtained a substantial decrease in the extents and rates of actin polymerization and a subsequent increase of the critical concentrations which were a function of antibody concentrations.

In the presence of preformed nuclei produced by low concentrations of gelsolin (gelsolin/actin ratio of 1/25 w/w), we also observed a decrease in the polymerization rate.

Finally, antibodies reacted well with either G-or F-actin. Their interaction with filamentous actin as well as the copolymerization of free actin and actin complexed with antibodies thus confirmed their effect on the elongation step by increasing the rate constant of dissociation k^-. In contrast, some sequestering proteins such as vitamin-D-binding protein did not at all bind with the filamentous form of actin [40].

If we consider now the three-dimensional model reported by Kabsch et al. [6], the 300–326 sequence, which includes the two concerned epitopes 1 and 3, presented a large temperature factor indicating a flexible structure. The flexible nature of the sequence would allow possible conformational modulations during actin polymerization or after effector binding (antibodies, Mg^{2+}).

Epitope 1 is implicated in the adenine site through its residues 303, 305 and 306. The nucleotide is located at a strategic position in a cleft between the two domains of the monomer and stabilises the actin structure. To obtain the best fit for their atomic model for filamentous actin, Holmes et al. [4] needed to twist subdomain 2 approximately 15° and the three other subdomains about 2–3° in the actin monomer. The G-actin would undergo structural motion involving changes in the relative positions of small and large domains as well as within each separate domain during polymerization. Moreover, the nature of the nucleotide (ATP or ADP) was recently shown to have a great influence on the flexibility of the actin filament [49]. Binding of an effector such as an Fab on the 300–306 sequence would therefore induce some structural constraints which could modify the actin–actin association parameters. We also observed that the binding of Mg^{2+} to F-actin affected its conformation in the same 300–306 region. If Ca^{2+} was substituted to Mg^{2+}, the effect was no longer observed which is indicative of the specific role of Mg^{2+} on low affinity binding sites [50]. These observations are in well agreement with recent studies giving evidence for the specific effect of Mg^{2+} towards a more flexible actin conformation [49].

Considering the turn where epitope 3 is located (Fig. 1) both the structural models of Holmes et al. [4] and Schmidt et al. [7] show that the 308–330 sequence (helix-turn-beta motif) is at the surface of the actin monomer in the filament and constitute most the front surface of subdomain 3. This sequence lies in the region which makes intermolecular interactions between three monomers [5]. In particular, the segment 322–328 including the Met 325 pointing to the inside of actin is adjacent to the 240–245 loop [5,7]. However, molecular dynamics stimulation (XFLOR) did not take into account the 318–328 and 240–245 sequences as possible contacts between monomers. In fact, the sequence 308–330 is accessible enough in the actin filaments to allow interaction of the 60K COOH terminal domain of scruin with 11 residues (namely residues 323, 326 and 328). Accordingly to the results of Schmid et al.[7] on the scruin–actin complex, we also observed a similar reactivity of anti-(epitope 3) antibody with the turn of sequence 320–328 in G-and F-actins. Therefore, the inhibitory effect afforded by anti-(epitope 3) antibody can be partly explained by the proximity with an actin–actin interacting region and not by a direct steric effect after antibody binding.

Another possible effect of the antibodies on actin conformation could be ascribed to the fact that antibodies were elicited using unfolded forms of actin or actin fragments and subsequently could induce some structural distortions in this actin region.

The functional importance of the 300–326 sequence is substantiated by its involvement in the interface of several actin binding proteins, i.e. gelsolin tropomyosin and scruin which modulate the conformational and polymerization states of actin. Thus, the C-terminal half (S4–6 domains) of gelsolin upon interaction at the 305–326 sequence [14,51,52] impedes actin polymerization. In contrast, scruin by its binding both with the 308–330 sequence of actin and with the 112–136 sequence in an adjacent

monomer stabilizes and rigidify the actin filament [7].

In conclusion, the loop–helix–loop structure in subdomain 3 (i.e. 300–326 sequence) located at the outside surface of actin filament corresponded to an important functional site correlated with actin polymerization, and binding of low affinity divalent cations.

Acknowledgements

We thank Dr. D. Pantaloni for his critical reading of the manuscript and helpful comments. This work was supported by grants from the 'Association Française contre les Myopathies' and the IFREMER and a scholarship to A.H. from the 'Ministère de l'Education Nationale de Mauritanie'.

References

[1] J.F. Rouayrenc and F. Travers, Eur. J. Biochem., 116 (1981) 73–77.
[2] S. Rich and J. Estes, J. Mol. Biol., 104 (1976) 777–792.
[3] C. Roustan, Y. Benyamin, M. Boyer, R. Bertrand, E. Audemard and J. Jauregui-Adell, FEBS Lett., 181 (1985) 119–123.
[4] K. Holmes, D. Popp, W. Gebhard and W. Kabsch, Nature, 347 (1990) 44–49.
[5] M. Lorenz, D. Popp and K.C. Holmes, J. Mol. Biol., 234 (1993) 826–836.
[6] W. Kabsch, H.G. Mannherz, D. Suck, E. Pai and K. Holmes, Nature, 347 (1990) 37–44.
[7] M.F. Schmid, J.M. Agris, J. Jakana, P. Matsudaira and W. Chiu, J. Cell Biol., 124 (1994) 341–350.
[8] R.R. Schröder, D.J. Maresteni, W. Jahn, H. Holden, I. Rayment, K.C. Holmes and J.A. Spudich, Nature, 364 (1993) 171–174.
[9] C.E. Schutt, J.C. Myslek, M.D. Rozycki, N.C.W. Goonesekue and U. Lindberg, Nature, 365 (1993) 810–816.
[10] P.J. McLaughlin, J.T. Gooch, H.G. Mannherz and A.G. Weeds, Nature, 364 (1993) 685–692.
[11] J.A. Spudich and S. Watt, J. Biol. Chem., 246 (1971) 4866–4871.
[12] P. Detmers, A. Weber, M. Elzinga and R. Stephens, J. Biol. Chem., 256 (1981) 99–105.
[13] T. Kouyama and K. Mihashi, Eur. J. Biochem., 114 (1981) 33–38.
[14] A. Houmeida, V. Hanin, J. Feinberg, Y. Benyamin and C. Roustan, Biochem. J., 274 (1991) 753–757.
[15] Z. Soua, F. Porte, M.C. Harricane, J. Feinberg and J.P. Capony, Eur. J. Biochem., 153 (1985) 275–287
[16] J.P. Labbé, M. Boyer, C. Roustan and Y. Benyamin, Biochem. J., 284 (1992) 75–79.
[17] A. Houmeida, V. Hanin, J. Constans, Y. Benyamin and C. Roustan, Eur. J. Biochem., 203 (1992) 499–503
[18] Y. Benyamin, C. Roustan and M., Immunol. Methods, 86 (1986) 21–29.
[19] V. Hanin, Doctorat thesis, Montpellier, France, 1990, pp. 73–88.
[20] Y. Benyamin, C. Roustan, M. Boyer, C. Mejean, J. Feinberg and J.P. Labbe, in Sarcomeric and Non-Sarcomeric Muscles: Basic and Applied Research Prospects for the 90's, Unipress, Padova, 1988, pp. 113–118.
[21] A. Houmeida, Doctorat thesis, Montpellier, France, 1991, pp. 72–84.
[22] M. Boyer, C. Roustan and Y. Benyamin, Biosci. Rep., 5 (1985) 39–46.
[23] M. Boyer, J. Feinberg, H.K. Hue, J.P. Capony, Y. Benyamin and C. Roustan, Biochem. J., 248 (1987) 359–364.
[24] C. Mejean, H.K. Hue, F. Pons, C. Roustan and Y. Benyamin, Biochem. Biophys. Res. Commun., 152 (1988) 368–375.
[25] J. Vandekerckhove, H-G. De Couet and K. Weber, Molecular evolution of muscle-specific actins: A protein-chemical analysis, in C.G. Dos Remedios and J.A. Barden (Editors), Actin Structure and Function in Muscle and Non Muscle Cells, Academic Press, New York, 1983, pp. 241–248.
[26] C. Mejean, F. Pons, C. Roustan and Y. Benyamin, Biochem. J., 264 (1989) 671–677.
[27] H.K. Hue, Y. Benyamin and C. Roustan, J. Muscle Res. Cell Motil., 10 (1989) 135–142.
[28] K. Anderson, Y. Benyamin, C. Douzou and C. Balny, J. Immunol. Methods, 23 (1978) 17–21.
[29] G.M. Edelman and J.J. Marchalonis, in C.A. Williams and M.W. Chase (Editors), Methods in Immunology and Immunochemistry, Vol. 1, Academic Press, New York, 1967, pp. 418–420.
[30] C. Mejean,, M.C. Lebart, M. Boyer, C. Roustan and Y. Benyamin, Eur. J. Biochem., 209 (1992) 555–562.
[31] M-F. Carlier, D. Pantaloni and E. Korn, J. Biol. Chem., 260 (1985) 6565–6571.
[32] C. Frieden, Proc. Natl. Acad. Sci. USA, 80 (1983) 6513–6517.
[33] L.S. Tobacman and E.D. Korn, J. Biol. Chem., 258 (1983) 3207–3214.
[34] R. Fesce, F. Benfenati, P. Greengard and F. Valtorta, J. Biol. Chem., 267 (1992) 11289–11299.
[35] J.A. Cooper and T.D. Pollard, Methods Enzymol., 85 (1982) 182–270.
[36] U.K. Laemmli, Nature (London), 227 (1970) 680–685.
[37] T.D. Pollard and S.W. Craig, TIBS, 7 (1982) 55–58.
[38] E.D. Korn, Physiol. Rev., 62 (1982) 672–737.
[39] M–F. Carlier, J. Biol. Chem., 266 (1991) 1–4.
[40] M. Coué, J. Constans and A. Olomucki, Eur. J. Biochem., 160 (1986) 273–277
[41] Y. Doi and C. Frieden, J. Biol. Chem., 259 (1984) 11868–11875.
[42] W. Kabsch and J. Vandekerckhove, Ann. Rev. Biophys. Biomol. Struct., 21 (1992) 49–76.

[43] A. Lees, J. Haddad and S. Lin, Biochemistry, 23 (1984) 3038–3047.
[44] T.C. Tsang, FEBS Lett., 323 (1993) 1–3.
[45] R. Sauterer, R. Eddy, A. Hall and J. Condeelis, J. Biol. Chem., 266 (1991) 24533–24539.
[46] L. Miller, M. Phillips and E. Reisler, J. Biol. Chem., 263 (1988) 1996–2002.
[47] J. Janin and C. Chothia, J. Biol. Chem., 265 (1990) 16027–13030.
[48] G., Dasgupta, J. White, M. Phillips, J. Bulinski and E. Reisler, Biochemistry, 29 (1990) 3319–3324.
[49] A. Orlova and E.H. Egelman, J. Mol. Biol., 227 (1992) 1043–1053.
[50] M.F. Carlier, D. Pantaloni and C.D. Holmes, J. Mol. Biol., 261 (1986) 10778–10784.
[51] D. Kwiatkowski, P. Janmey, J. Mole and H. Yin, J. Biol. Chem., 260 (1985) 15232–15238.
[52] M. Way, J. Gooch, B. Pope and G. Weeds, J. Cell Biol., 109 (1989) 593–605.